CHAPTER III

THEORETICAL CONSIDERATIONS

3.1 Basic Principles of Catalysis [26]

3.1.1 Definitions

3.1.1.1 Catalyst

The basic concept of catalyst is that of a *substance that in small amount causes a large change*. More precise definitions of catalysis and of what constitutes a catalyst have gradually evolved as understanding of the causes of catalytic phenomena has grown. Even today there is no universal agreement on definitions, the point of view varying somewhat depending upon the investigator; for example, as between the fundamental investigator and the practitioner, and among researchers concerned with heterogeneous catalysis, homogeneous catalysis, polymerization reactions, and enzymes. For present purposes however our definition is: *A catalyst is a substance that increases the rate of reaction without being appreciably consumed in the process.*

A catalyst *cannot* change the ultimate equilibrium determinated by thermodynamics; its role is restricted to accelerating the rate of approach to equilibrium.

3.1.1.2 Catalyst Activity

The *activity* of a catalyst refers to the rate at which it causes the reaction proceed to chemical equilibrium. The rate may be expressed in any of several ways. The performance of an industrial reactor is frequently given in terms of a space-time yield (STY), which is the quantity of product formed per unit time per unit volume of reactor.

3.1.1.3 Sites

Under reaction conditions all solid catalysts are nonuniform or heterogeneous in the sense that chemical and physical properties will vary with location on the surface. Even in a pure metal the atoms at specific locations, such as at lattice defects and at edges and corners of crystallites, are different from atoms in a surface plane. The heterogeneity of catalyst surfaces can be demonstrated and to some extent characterized by a variety of methods. The variation of the differential heat of adsorption with coverage or the change in activation energy of adsorption with coverage may be measured, or temperature-programmed desorption studies may be used. More than one maximum in chemisorption isotherms may be observed (Fig. 3.1), showing that more than one kind of chemisorption may occur. Some catalysts may be effectively poisoned by adsorption of an amount of material comprising much less than a monolayer, demonstrating that only a fraction of such a surface is effective for reaction.

These facts and others led to the concept, introduced by H.S. Taylor (1984), that reaction take places only on specific locations on the catalyst, termed *sites*. Those that are active for one reaction may not be so for a second reaction, but it is usually difficulty to identify their identity and structure precisely. In some cases a site may be a group or cluster of neighboring atoms on the catalyst surface; sometimes it may actually be a species adsorbed onto the catalyst. The term *active center* is frequently used as a synonym for *site*, or to refer to a group of sites. A catalyst will frequently undergo reconstruction during reaction, causing a change in total area and nature of the surface and possibly a change in number and nature of the sites. For some reactions on metals the rate is independent of the site, shape, of other physical characteristics of the metal crystallite and is proportional only to the total number of metal atoms exposed to the reactant (this is typically about 10^{15} atoms per square centimeter). Such reactions are termed *structure-insensitive* in contrast to *structure-sensitive* reactions whose rates do vary with the detailed structure of the surface. The terms *facile* for *structure-insensitive* and *demanding* for *structure-sensitive* are also used. The concentration of active sites on acid catalysts is usually much less than that on metals and is typically of the order of magnitude of about 10^{11} sites per square centimeter.

3.1.2 Kinetics of Catalytic Reactions [27]

The primary effect of a catalyst on a chemical reaction is thus to increase its rate, and this must mean to increase its rate coefficient. The consequential effects may be analysed in terms of either the collision theory or the absolute rate theory.

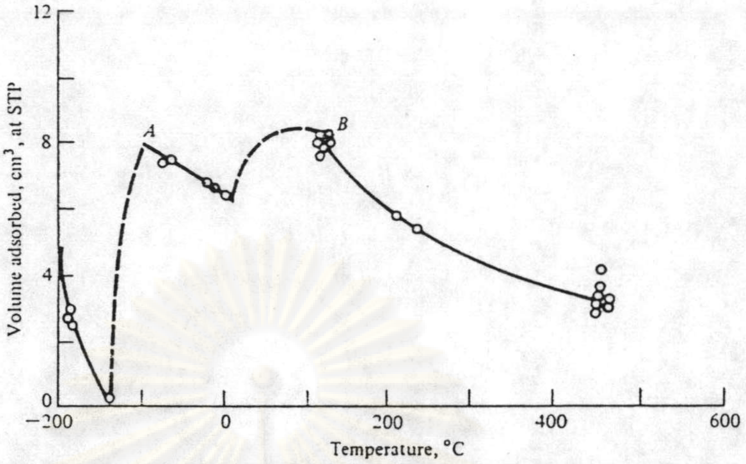

Figure 3.1 Adsorption isobar of hydrogen at atmospheric pressure on an iron catalyst used in the synthesis of ammonia, showing maxima corresponding to two types of chemisorptions. (Emmett and Harkness, 1935)

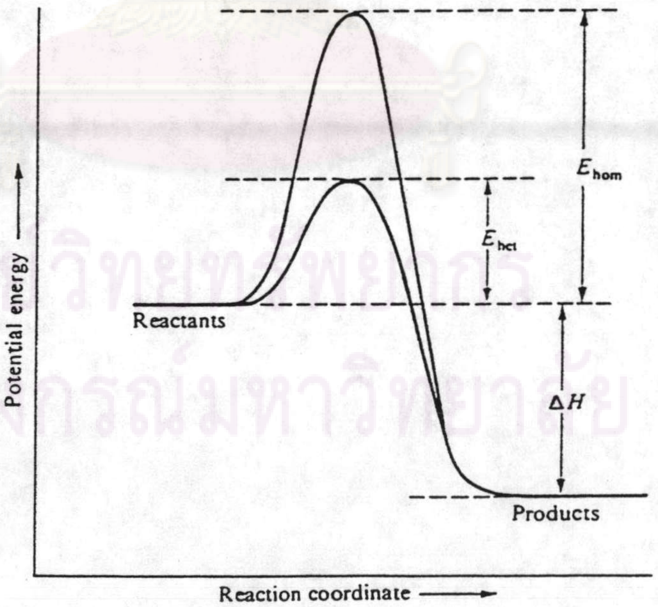

Figure 3.2 Potential energy profile for an exothermic reaction, showing the lower activation energy of the catalytic reaction.

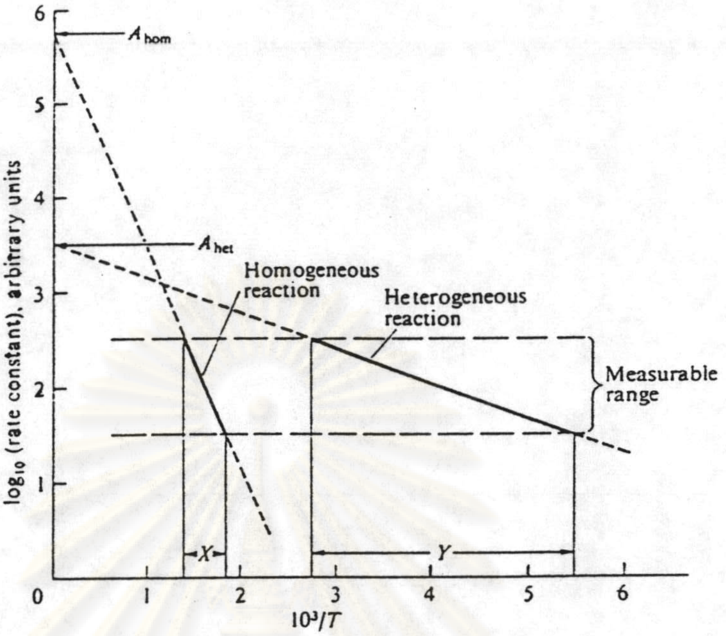

Figure 3.3 Arrhenius diagram for uncatalytic and catalytic reactions: X and Y are the ranges of 1/T in which the respective reactions can be observed.

According to the collision theory, the rate coefficient k is given by

$$k = Pz \exp(-E/RT)$$

where P is the so-called steric factor, z the collision frequency, R the gas constant and T the absolute temperature. Let us consider, for example, a unimolecular transformation (A $\longrightarrow$ B) in which the slow step is the adsorption of the reactant: the collision frequency in question is then the number of collisions per unit time between the reactant molecules and the catalytic sites or species. Now the concentration of the latter will be quite small and so the number of relevant collisions will be much smaller (by a factor of some 10^{12}) than the number of collision between reactant molecules alone, which is relevant to the uncatalytic reaction but irrelevant to the catalytic reaction. Therefore if the catalytic reaction is to complete effectively with the uncatalytic reaction, then its exponential term must be some 10^{12} times larger, which means that its activation energy must be about 65 kJ mol^{-1}less. There may be some small relief in the form of a higher steric factor but this is unlikely to contribute more than a factor of 10^{2} or 10^{3} at most, and the main conclusion is not really altered. Neglecting this effect, we see that an activation energy difference of 65 kJ mol^{-1}only makes the rates of catalytic and uncatalytic reactions equal: this scarcely represents efficient catalysis, for which the activation energy difference typically must exceed 100 kJ mol^{-1}.

In terms of the absolute rate theory, the rate coefficient is given by

$$k = (kT/h)\ \exp(-\triangle G^{+}/RT)$$

where **k** is the Boltzmann constant, $\triangle G^{+}$ is the Gibbs free energy of activation and h is Planck's constant, and so that effect of a catalyst must be to decrease the free energy of activation of the reaction. This in turn is composed of an entropy and an enthalpy of activation. Now the entropy of activation in a catalytic reaction will usually be less than in the corresponding uncatalytic reaction because the transition state is immobilized on the catalyst surface with consequent loss of translational freedom. There must therefore be a corresponding decrease in the enthalpy of activation to compensate for this, or more than to compensate if efficient catalysis is desired. Thus according to either theory, the activation energy for a catalytic reaction ought to be less than for the same uncatalytic reaction. There is much experimental evidence to show that such is indeed the case: some values of activation energies for catalytic and uncatalytic reactions are given in Table 3.1.

Table 3.1 Activation energies (kJ mol^{-1}) for uncatalytic and catalytic reactions

Reaction	E (uncatalytic)	E (catalytic)	Catalyst
$2HI \longrightarrow H_2 + I_2$	184	-	-
	-	105	Au
	-	59	Pt
$2N_2O \longrightarrow 2N_2 + O_2$	245	-	-
	-	121	Au
	-	134	Pt
Pyrolysis of $(C_2H_5)_2O$	224	-	-
	-	144	I_2 vapour

This situation may be shown both as a potential-energy profile (Figure 3.2) and as an Arrhenius diagram (Figure 3.3): the latter makes it plain that the effect of a catalyst is either to increase the rate coefficient at a given temperature (except at very high temperatures) or to decrease the temperature at which it achieves a given value. Some care is necessary in drawing precise comparisons between homogeneous and heterogeneous reactions. For example, the dimensions of the rate coefficients and of the pre-exponential factors differ, and this affects their values:

furthermore the value of the pre-exponential factor for a catalytic reaction depends on the active surface area of the catalyst. It must however be emphasized that *the lowering of the activation energy is a fundamental principle of catalysis*, and that it applies to all forms of catalysis-homogeneous, heterogeneous, and enzymatic.

3.1.3 Classification of Catalytic Systems

The above remarks apply indiscriminately to all forms of catalysis: they are the universal validity wherever catalysis occurs. In fact it is possible to divide catalytic systems into two distinct categories. When the catalyst is of the same phase as the reactants and no phase boundary exists, we speak of *homogeneous catalysis*. This may take place either:

(a) in the gas phase, as, for example, when nitrogen oxide catalyses the oxidation of sulfur dioxide; or

(b) in the liquid phase, as when acids and bases catalyse the mutarotation of glucose.

When a phase boundary separates the catalyst from the reactants, we speak of *heterogeneous catalysis*. A number of phase combination can then occur, as shown in Table 3.2. Other possible phase combinations rarely arise in catalysis.

There is however one extremely important group of substances which cannot be accommodated within this classification. *Enzymes* are neither homogeneous nor heterogeneous catalysts; they are large complex organic molecules, usually protein, which form a lyophilic colloid: this is neither a homogeneous nor a heterogeneous system, but something in between. We must therefore regard enzymatic catalysis as something quite different from the other two forms of catalysis. However, it is not within the scope of this thesis to discuss enzymatic catalysis in any detail.

3.1.4 Classification of Solid Catalysts

When industrial scientists are called upon to devise a catalyst for a new application, they must have the basic information they need in a readily accessible form. As the process of catalyst design becomes progressively more sophisticated with the increasing standards that are placed on a successful catalyst, so that chemical and physical complexity of the finished product becomes greater. If we know in general terms the most important capabilities of various classes of substances, it becomes easier to select the ingradients for an effective catalyst.

Table 3.2 Phase combinations for heterogeneous catalysis

Catalyst	Reactant	Example
Liquid	Gas	Polymerization of alkenes catalysed by phosphoric acid
Solid	Liquid	Decomposition of hydrogen peroxide catalysed by gold
Solid	Gas	Ammonia synthesis catalysed by iron
Solid	Liquid+Gas	Hydrogenation of nitrobenzene to aniline catalysed by palladium

Catalysis is essentially a chemical phenomenon. The ability of a substance to act as a catalyst in a specified system depends on its chemical nature. With heterogeneous catalysis we are concerned with the specific chemical properties of the surface of the chosen substance. These of course reflect the chemistry of the bulk solid, and some useful insight into the catalytic activities of surface is gained from knowledge of the bulk properties of the solid. Our first objective must be to try to understand in general terms how the type of reaction best catalysed by a solid depends on its chemical nature.

Table 3.3 Classification of heterogeneous catalysts (less important functions in parentheses)

Class	Functions	Examples
Metal	hydrogenation dehydrogenation hydrogenolysis (oxidation)	Fe, Ni, Pd, Pt, Ag
Semiconducting oxides and sulphides	oxidation dehydrogenation desulphurization (hydrogenation)	NiO, ZnO, MnO_2, Cr_2O_3, Bi_2O_3-MoO_3, WS_2
Insulator oxides	dehydration	Al_2O_3, SiO_2, MgO
Acids	polymerization isomerization cracking, alkylation	H_3PO_4, H_2SO_4, SiO_2-Al_2O_3, zeolites

Table 3.3 present a preliminary and somewhat superficial classification of solids into groups depending on their catalytic activities. This table may be in part interpreted using the qualitative concept of *compatibility* between catalysts, reactants, and products. For catalysis to occur, there must be a chemical interaction between catalyst and the reactant-product system, but this interaction must not change the chemical nature of the catalyst except at the surface. Thus by compatibility we mean the existence of a surface interaction which does not penetrate into the interior of the solid.

Table 3.3 shows that transition metals especially good catalysts for reactions involving hydrogen and hydrocarbons. This is because these substances readily *adsorb* at the surfaces of metals, in a manner to be described in more detail below, and except in a few cases the reaction does not proceed below the surface. Base metals are useless as catalysts for oxidation because at the necessary temperature they are rapidly oxidized throughout their bulk. Only those 'noble' metals (such as palladium, platinum and silver) that are resistant to oxidation at the relevant temperature may be used as oxidation catalysts. Many oxides on the other hand are excellent oxidation catalysts because they interact with oxygen and other molecules, but with some important exception, i.e. copper chromium oxide $Cu^{II}Cr_2^{III}O_4$ ('copper chromite') they are not well suited for hydrogenation because of the likelihood of reduction to metal. Those oxides which may be for hydrogenation or dehydrogenation are of course immune to reduction by hydrogen at the temperature at which they are active. Similarly metal sulphides catalyse reactions of molecules containing sulphur: if oxides such as alumina, silica, and magnesia which do not interact much with oxygen are poor oxidation catalysts, but they easily adsorb water and thus may be used to catalyse dehydration. The concept emerges that we must first understand the adsorption of molecules at solid surfaces before we can proceed to a deeper knowledge of catalysis.

3.2 Carbon Monoxide and Its Chemistry [28,29]

3.2.1 Introduction

Carbon monoxide (CO), a colourless, odorless, flammable, toxic gas, is produced by steam reforming or partial oxidation of carbonaceous materials. It is used as a fuel, a metallurgical reducing agent, and a feed stock in the manufacture of a variety of chemicals, notably methanol, acetic acid, phosgene, and oxo alcohols. Increased usage of carbon monoxide from coal in chemicals and fuels manufacture is likely if economic coal gasification technology evolves.

Carbon monoxide was discovered by Lassonne in 1776 by heating a mixture of charcoal and zinc oxide. It provided a source of heat to the industry and home as a component of town gas and was used as a primary raw material in German synthetic fuel manufacture during World War II; its compounds with transition metals were studied extensively in the rebirth of modern inorganic chemistry in the 1960s. Most recently, carbon monoxide emission from vehicle exhausts has been recognized as a primary source of air pollution.

3.2.2 The Structure and Chemical Properties

Proposals purporting to explain the structure of carbon monoxide are almost as old as organic chemistry itself. Pauling suggested that carbon monoxide could be represented by three important resonance forms each of which made an approximately equal contribution to the normal state of the molecule as follows:

$$\overset{+}{:C}:\overset{-}{O}: \qquad :C::\ddot{O}: \qquad \overset{-}{:C}:::\overset{+}{O}:$$

(a) (b) (c)

The triple bonded structure (c) is currently thought to be the most important structure and the one best describing carbon monoxide. According, the evidence for this structure will be discussed first.

The carbon monoxide molecule contains 14 electron; six contributed by carbon and eight by oxygen. In the ground state, the electron distribution in carbon is $1s^2 2s^2 2p^2$, and the eight electron of oxygen are distributed as $1s^2 2s^2 2p^4$. A triple bond may be formed between carbon and oxygen by the transfer of one p electron from the oxygen atom in which it is paired, to the vacant p orbital in carbon. The transfer produces two ions with identical electronic structures:

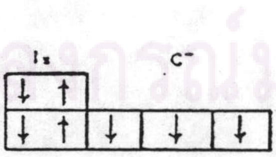

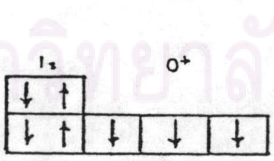

This structure may be represented as $\overset{-}{:C}:::\overset{+}{O}:$ in which only the valence (L shell) electrons are shown, or by the equivalent formulation $C\equiv O$, in which the formal charges are not shown and the coordinate bond (formed by a transfer of one electron from oxygen to carbon and giving rise to a shared pair in which both electrons are contributed by oxygen) is shown by the familiar arrow. The transfer of the electron produces a structure with three covalent bonds; additional stability is provided by the coulombic interaction of the oppositely charged atoms.

The bonding between carbon and oxygen in carbon monoxide is the best described by molecular orbital theory. The ten valence electrons from carbon and oxygen fill the lowest energy orbitals of carbon monoxide (^{b}, bonding; *, antibonding) to give the electronic configuration $(\sigma_s^b)^2 (\sigma_s^*)^2 (\pi_{xy}^b)^4 (\pi_z^b)^2$, which predicts one σ-and two π-bonds. The π^* and σ^* orbital of molecular carbon monoxide remain unfilled but available for bonding with transition metal atoms. The bond energy of 1070 kJ/mol (255.7 kcal/mol) is consistent with the triple bond formulation and is the highest observe bond energy for any diatomic molecules. The fundamental adsorption in the infrared spectrum of carbon monoxide is located at 2143 cm^{-1}.

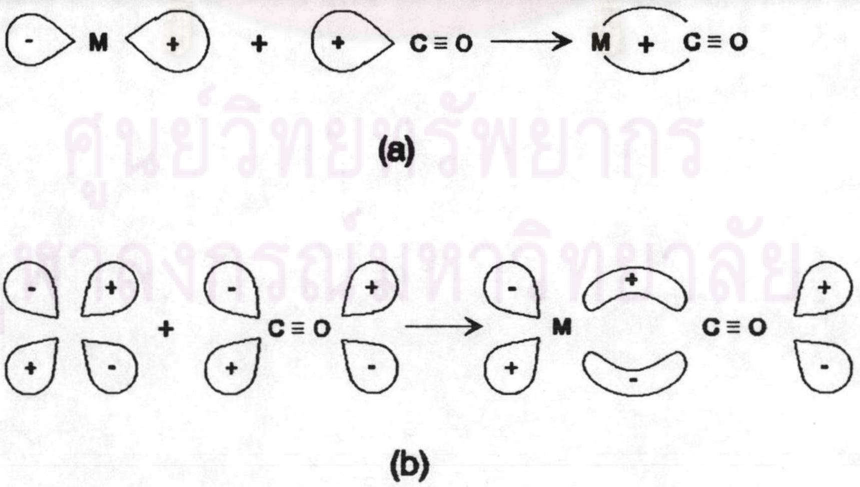

Figure 3.4 (a) Formation of a σ-bonding between a transition metal and carbon monoxide. (b) Metal-to-carbon monoxide π-bond formation.

The bonding between carbon monoxide and transition metal atoms is particularly important because transition metals, whether deposited on solid supports or present as discrete complexes, are required as catalysts for the reaction between carbon monoxide and most organic molecules. A metal-carbon σ-bond forms by overlapping of metal d-σ orbitals with σ orbitals on carbon. Multiple bond character between the metal and carbon occurs through formation of a metal-to-CO π-bond by overlap of a metal d-π orbital with the empty antibonding orbital of carbon monoxide (Figure 3.4). A weakened carbon-oxygen bond results from the combined σ- and π-bonding, allowing the metal-bonded carbon monoxide to react more readily.

3.2.3 Chemical Reaction of Carbon Monoxide

The examples of industrially significant reactions of carbon monoxide were performed as follows:

- **Water Gas Shift Reaction**

Carbon monoxide reacts with water over a catalyst to produce hydrogen and carbon dioxide. This reaction is used to prepare high purity hydrogen or synthesis gas with a higher hydrogen-to-carbon monoxide ratio than the feed.

$$CO + H_2O \longrightarrow H_2 + CO_2$$

- **Oxidation**

Carbon monoxide can be oxidized without a catalyst or at a controlled rate with a catalyst. Carbon monoxide oxidation proceeds explosively if the gases are mixed stoichiometrically and then ignited. Surface burning will continue at temperatures above 900 °C, but the reaction is slow below 650 °C without a catalyst. However, the reaction has been found to be catalysed at lower temperatures by many oxides such as CuO, NiO, MnO_2.

$$CO + 1/2\ O_2 \longrightarrow CO_2$$

- **Disproportionation**

Carbon monoxide readily disproportionates into elemental carbon and carbon dioxide on a catalyst surface.

$$2\ CO \longrightarrow C + CO_2$$

This decomposition is thermodynamically favored by decreasing temperature and increasing pressure. Decomposition is extremely slow below 400 °C in the absence of a catalyst; however, between 400-600 °C many surfaces, particularly iron, cobalt, and nickle, promote the disproportionation reaction.

- **Methanol**

Methanol is manufactured by the reaction between carbon monoxide and hydrogen at 230-400 °C and 5-60 MPa (50-600 atm). The reaction is extremely exothermic, and plants must be designed to remove heat efficiently.

$$CO + 2\ H_2 \longrightarrow CH_3OH$$

- **Acetic Acid**

Manufacture of acetic acid by methanol carbonylation has become a leading commercial route to acetic acid.

$$CH_3OH + CO \longrightarrow CH_3COOH$$

At one time acetic acid was manufactured by methanol carbonylation using an iodide-promoted cobalt catalyst, but vigorous conditions of temperature and pressure (220 °C, 48 MPa or 474 atm) were required to achieve yields of up to 60 %. In contrast, an iodide-promoted, homogeneous rhodium catalyst operates at 175-195 °C and pressure of 3 MPa (30 atm). These conditions dramatically lower the specifications for pressure vessels. Yields of 99 % acetic acid based on methanol are readily attained.

- **Fischer-Tropsch**

Carbon monoxide is catalytically hydrogenated to a mixture of straight-chain aliphatic, olefinic, and oxygenated hydrocarbon molecules in the Fischer-Tropsch reaction.

$$n\,CO + 2n\,H_2 \longrightarrow -(CH_2)_n- + n\,H_2O$$

The Fischer-Tropsch process was developed in Germany to manufacture synthetic gasoline during World War II. Carefully promoted iron and cobalt catalysts operating at conditions varying from 190-350 °C and 0.7-20 MPa (7-200 atm) were used. Depending on the specific operating conditions, products containing up to 75 % liquid hydrocarbon or 55 % oxygenated organic molecules were obtained.

3.3 Oxidation of Carbon Monoxide

3.3.1 Introduction

The early investigations of the mechanism of this oxidation forms one of the classical examples of researches in the field of heterogeneous catalysis. Stone [30] has pointed out that although an irreversible chemisorption in which a surface carbonate ion is produced explain the facts in the temperature range 100-200 °C; other processes have to be invoked to explain the catalytic oxidation of CO at 20 °C. The fact that CO_2 could be removed from the catalyst after a low-temperature oxidation was not consistent with an interpretation of experimental results in terms of a simple Langmuir-Hinshelwood mechanism, since CO_2 does not inhibit the reaction. Furthermore, although adsorbed CO_2 seems to be a stable state during a low-temperature catalytic oxidation, such a stable surface state cannot be reached simply by admitting CO_2 gas to the outgassed metal oxide catalyst.

It is instructive to discuss first the adsorption of CO at metal oxides and subsequently the oxidation of CO at both high and low temperatures, since it will emerge that there is a strong correlation between catalytic activity and the stability of adsorbed species.

3.3.2 Adsorption of Carbon Monoxide

The earliest experiments on the adsorption of CO on the oxide of zinc, chromium and manganese established that the gas could be adsorbed in two distinct ways. At room temperature, CO was adsorbed reversibly on ZnO and the gas could be recovered without change on heating the oxide to about 100 °C. The heat of adsorption, as measured by calorimetric experiment, was between 10 and 20 kcal mole^{-1}, so that chemisorption rather than physical adsorption was occuring [31]. On the oxides Mn_2O_3 and Mn_2O_3-Cr_2O_3, CO was irreversibly adsorbed in the sense that CO_2 was desorbed on heating. The heat of adsorption was over 30 kcal mole^{-1} and a considerable amount of oxygen could be adsorbed after CO adsorption in spite of the fact that little was adsorbed prior to CO adsorption [32]. This unsaturation towards oxygen was carefully measured and it was found that the quantity of oxygen take up amounted to about one-half of the amount of presorbed CO. In conjunction with the calorimetric data, summarized in Table 3.4.

It was possible to postulate a mechanism of adsorption and oxidation involving the CO_3^{2-} surface complex. Table 3.4 shows that the same adsorbed state is probably reached when oxygen is admitted subsequent to CO adsorption and also when a mixture of $2CO:1O_2$ is adsorbed at an oxidized surface. Furthermore, if the heat of adsorption of CO_2 is subtracted from the quantity (Q_{CO} + $1/2Q_{O(s)}$), which represents the sum of (i) the heat of adsorption of CO and (ii) the heat of adsorption of oxygen on a surface at which CO had been presorbed, then the resulting value 65 kcal mole^{-1} is in close agreement with the heat of combustion of CO (g). Noting that the heat of adsorption of CO_2 on Mn_2O_3 corresponds very closely with the heat of dissociation of manganous carbonate, it was concluded that the adsorbed state common to these processes is a surface carbonate ion. It was supposed that the CO interacted with an oxygen ion of the metal oxide lattice, producing

Table 3.4 Heats of adsorption on $Mn_2O_3.Cr_2O_3$

Heat of adsorption of CO, Q_{CO}	46 kcal $mole^{-1}$
Heat of adsorption of O_2 after presorbing CO, Q_{O2}	78 kcal $mole^{-1}$
$Q_{CO} + 1/2\ Q_{O2}$	85 kcal $mole^{-1}$
Heat of adsorption of a mixture of 1 mole of CO and 1/2 mole of O_2, $Q_{(CO+1/2O2)}$	85 kcal $mole^{-1}$
Heat of adsorption of CO_2, Q_{CO2}	20 kcal $mole^{-1}$

the surface carbonate ion, and that unsaturation towards oxygen after CO adsorption occurred as a result of an anion vacancy produced by the CO adsorption. The process is represented by Garner [31] as:

$$\begin{array}{ccccc} M^{2+}\ O^{2-}\ M^{2+} & CO & M^{2+}\ O^{2-}\ M^{2+} & 1/2O_2 & M^{2+}\ CO_3^{2-}\ M^{2+} \\ O^{2-}\ M^{2+}\ O^{2-} & \xrightarrow{\hspace{2em}} & O^{2-}\ M^{2+}\ 2e & \xrightarrow{\hspace{2em}} & O^{2-}\ M^{2+}\ O^{2-} \end{array}$$

For p-type oxides (e.g. Cu_2O), such an irreversible adsorption of CO will, cause a decrease in the number of positive holes, since those electrons released by formation of the surface complex will tend to associate themselves with Cu^{2+} - Cu^{+} positive hole units. The adsorption will therefore result in a decrease in semiconductivity and is depletive, since the electron released will gradually from a potential barrier to further adsorption. On the other hand, for n-type oxides the electron released by irreversible CO adsorption will enter the conduction band of the solid and result in an increase in conductivity. Since there are vacant levels present in the conduction band which enable the incorporation of more electrons, the adsorption will be cumulative.

More elaborate calorimetric experiments by Stone and co-worker [33,34,35] showed that, with cuprous oxide, pre-adsorption of oxygen considerably increased the heat of adsorption of CO. Similarly, pre-adsorption of CO enhanced the heat of adsorption of oxygen. The surface complex thus produced was stable in the presence of excess oxygen, but CO_2 was desorbed if excess CO was present. Experiments in which CO_2 was adsorbed provided confirmatory evidence that the surface complex has the formula CO_3. Only when there was some pre-adsorbed oxygen present at the surface was CO_2 adsorbed, and this was adsorbed in the greatest amounts when CO_2 and O_2 were premixed in the ratio 2:1 before adsorption. The equation can thus be written for the reaction between presorbed O_2 and CO_2;

$$1/2O_2\ (g) = O\ (ads) + 28\ \text{kcal} \tag{1}$$
$$CO_2\ (g) + O\ (ads) = CO_3\ (ads) + 21\ \text{kcal} \tag{2}$$

Using the accepted data for the heat of combustion of CO;

$$CO\ (g) + 1/2O_2\ (g) = CO_2\ (g) + 67\ \text{kcal} \tag{3}$$

it therefore follows, from Hess's law of heat conservation, that 60 kcal is liberated when CO is adsorbed on a surface containing presorbed oxygen;

$$(3)-(1)+(2);\ CO\ (g) + 2O\ (ads) = CO_3\ (ads) + 60\ \text{kcal} \tag{4}$$

This may be compared with the experimental value of 49 kcal. From the calorimetric data for the adsorption of CO on a baked-out surface;

$$\text{CO (g)} \quad = \quad \text{CO (ads)} + \quad 20 \text{ kcal} \qquad (5)$$

one therefore predicts that the heat of adsorption of CO on a surface containing presorbed oxygen is 96 kcal;

$$\{2X(1)+(4)-(5)\};\ O_2(g)+CO(ads) = \quad CO_3(ads) + \quad 96 \text{ kcal} \qquad (6)$$

in comparison with the 100 kcal $mole^{-1}$ obtained by calorimetry. These reactions were also studied at the surfaces of nickel oxide and cobalt oxide and similar results found. Oxygen was also admitted after CO adsorption had taken place and, as before, surface unsaturation towards oxygen was evident.

After CO adsorption, however, the surface would not adsorb any further quantities of oxygen. The results are therefore in accord with the view that CO_3 complex formation occurs by CO interaction with two surface oxygen atoms. A vacant surface site, which will display unsaturation towards oxygen, therefore remains unoccupied left according to this mechanism. CO_3 complex formation also occurs by CO_2 being adsorbed at a surface oxygen site, but in this case no vacancy remains and the surface will not be unsaturated with respect to oxygen. The essential difference between this mechanism and that of the theory proposed by Garner [31] is that no lattice oxygen ions have been invoked. The mechanism is represented;

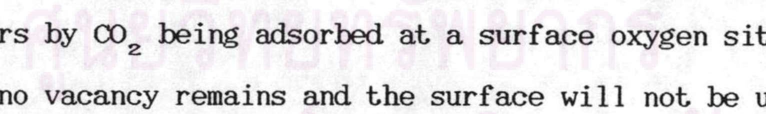

$$\begin{array}{ccccccccccccc} O & O & O & CO & & CO_3 & & O & 1/2O_2 & & CO_3 & O & O \\ | & | & | & & & | & & | & & & | & | & | \\ M & M & M & & \longrightarrow & M & M & M & & \longrightarrow & M & M & M \end{array}$$

Although it seems to be substantial evidence in favour of formation of a CO_3 surface complex, it remains doubt as to the exact role of lattice oxide ions. Winter [36] showed that when outgassed nickel oxide, prepared as an oxide film on a metal base, was exposed at 540 °C to oxygen containing ^{18}O, complete exchange of all the surface oxide ions of the oxide occurred. CO was then admitted to the oxide, now containing $^{18}O^{2-}$ ions, at 200 °C, and no measurable exchange of oxygen was observed. Similarly, CO_2 did not exchange its oxygen with the oxide ions of the solid. When a mixture of $2CO_2:1O_2$ was in contact with the solid at 50 °C the mixture was converted to CO_2, but only a small fraction of ^{18}O appeared in the gas phase. It seems, therefore, that for NiO at least, oxide ions of the lattice play no part in CO oxidation, as was assumed by Stone in the scheme outlined above.

Winter [14,36] also studied the exchange of oxygen with outgassed cuprous oxide and in this case found that both CO and CO_2 readily exchanged oxygen with the whole oxide surface at room temperature. And there was some exchange at temperature as low as -78 °C. Since there would not have been any adsorbed oxygen at the surface of the outgassed oxide, it must be assumed that both CO and CO_2 are adsorbed species is the carbonate ion, as originally propose by Garner. However, Stone postulates an alternative explanation in view of the difficulty of accounting for the energetics of dissociation of the carbonate ion to give desorbed CO, which is the stable gas-phase species remaining after the oxygen-exchange experiments. Cuprous oxide is a unique oxide, since it has a body-centred anion lattice with cations arranged in tetrahedral coordination around them. Figure 3.5 shows, diagrammatically, the arrangement of copper and oxygen ions in the (001) and (111) planes.

Half of the oxygen anions present at the surface protrude from the geometric plane containing the cuprous ions and half are buried beneath this plane.

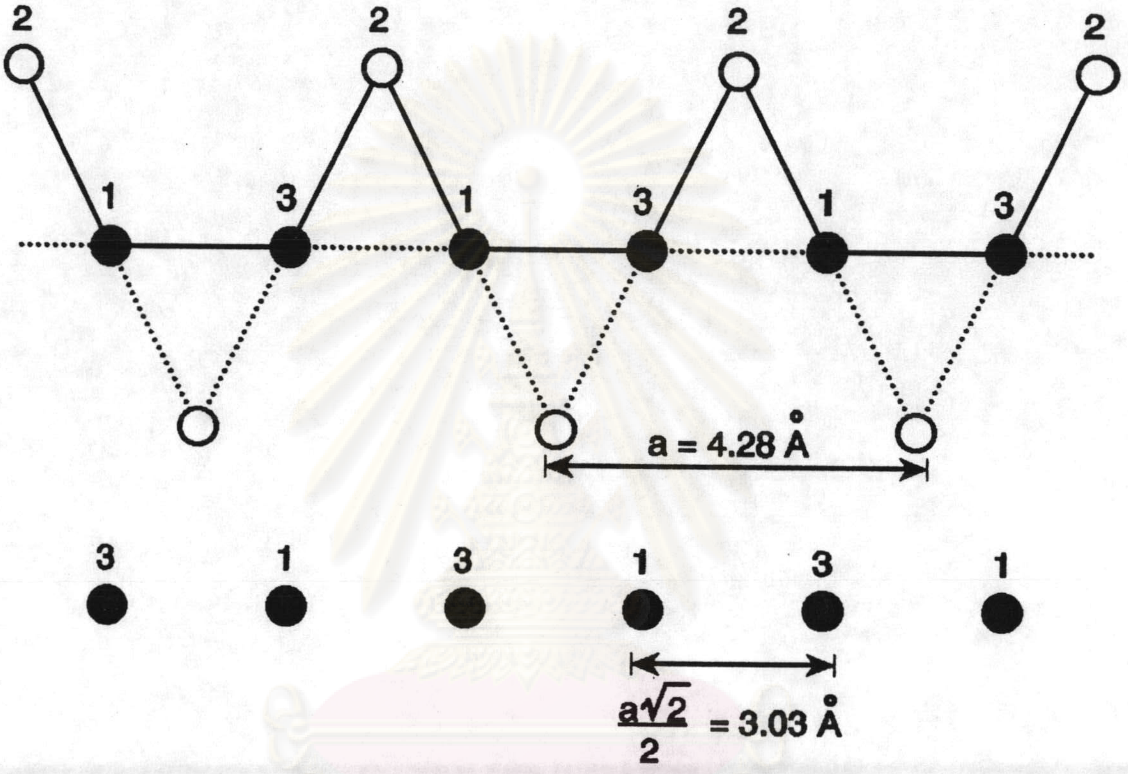

Figure 3.5 CO oxidation. Cross-section through a (001) plane of cuprous oxide; ○, oxygen atoms; ●, copper atoms.

Stone suggested that at temperature of 200°C, at with Winter outgassed his oxide, some of the oxygen ions in the "buried" position are converted to the "protruding" position and are thus favourably disposed for exchange with gas-phase atoms. Furthermore, there is hardly a distinction between such protruding oxygen anions and adsorbed oxygen. In the (011) plane, as depicted in Figure 3.6.

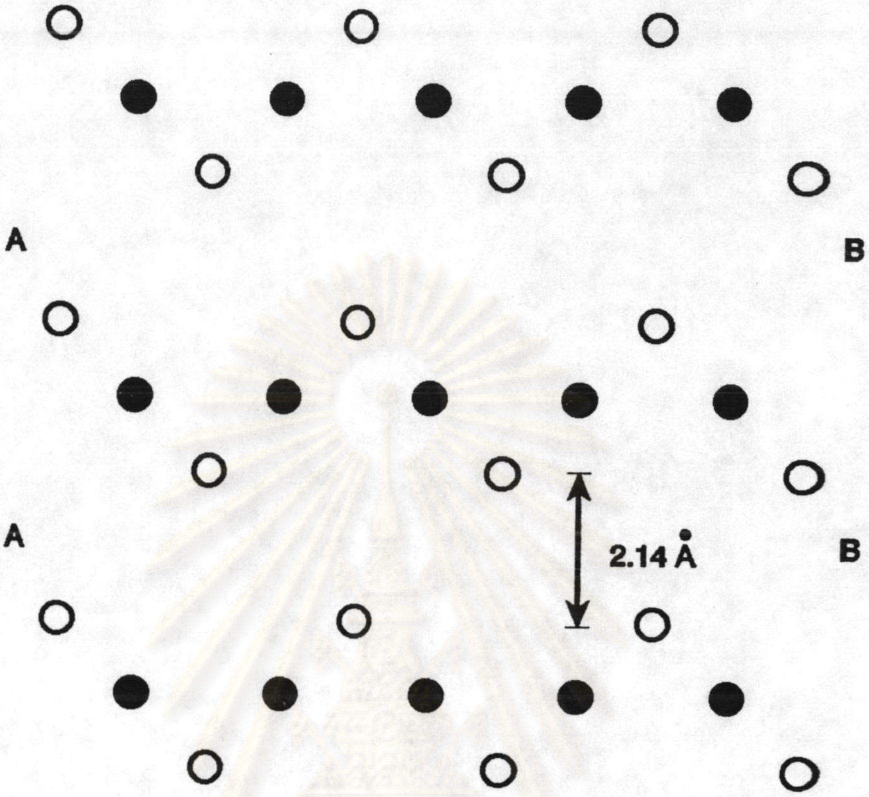

Figure 3.6 CO oxidation. Plane view of a (011) face of cuprous oxide. ○, oxygen atom; ●, copper atoms.

Oxygen ions are in suitable positions along AB for exchange with reversibly adsorbed CO or CO_2. Cuprous oxide therefore has such a geometric structure that one can reasonably expect oxygen to be exchanged with comparative ease at each of the three main geometrical planes. On the other hand, there are no favourably displaced oxygen ions in the NiO lattice and nickel ions in the flat (111) plane are somewhat inaccessible. Thus, it is understandable in these terms why there is a much lower activity in oxygen exchange with CO and CO_2 when NiO is used as opposed to Cu_2O. Further support for this argument comes from the work of Teichner [37,38] who found that CO and CO_2 exchanged oxygen with high specific surface area NiO which had not been sintered. If NiO is prepared in this way, it is to be expected that there will be an adequate number of oxygen ions suitably displaced for exchange with gaseous oxygen. Also, there is enhanced chemisorption of CO, and the labile oxide ions may again be responsible for this increase in activity.

The structure for the CO_3 complex proposed by Eischens and Pliskin, [39] using the technique of infrared spectroscopy, is of a form similar to a bicarbonate ion with binding to the metal atom through an oxygen atom, as shown below.

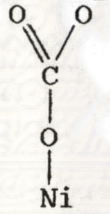

This structure is difficult to envisage in view of the previous evidence purporting to a carbonate type complex in which CO_2 is borned through an adsorbed oxygen ion. More recent evidence concerning the nature of the surface complex present under oxidation conditions is provided by the work of Blyholder [40]. Nickel was evaporated into an oil film and this was subsequently oxidized at the surface only and that an absorption band at 1330 cm^{-1}, additional to the ones detected by Eischens and Pliskin, appeared. By comparing the observed absorption bands with those shown by monodentate and bidentate carbonates, it was concluded that the spectra was more in accord with a surface carbonate complex than the structure proposed earlier.

3.3.3 Mechanism of Oxidation of Carbon Monoxide

At temperature of about 25°C, a mechanism involving the CO_3 complex explains the observed fact;

$$CO\ (g) = CO\ (ads) \qquad (7)$$

$$O_2\ (g) = 2O\ (ads) \qquad (8)$$

$$CO\ (ads) + 2O\ (ads) = CO_3\ (ads) \qquad (9)$$

$$CO_3(ads) + CO\ (g) = 2CO_2\ (g) \qquad (10)$$

If the catalyst is evacuated after oxidizing CO, then the steady state concentration of CO_3 (ads) remains unaltered, but if the catalyst is strongly outgassed carbon dioxide and oxygen are desorbed, as would be expected. A novel feature of this mechanism is that the product of reaction can actually enhance formation of the intermediate surface complex. The complex CO_3 may be attained by gaseous CO_2 reaction with adsorbed oxygen, as shown by equation (2). However, there exists some evidence [14] to show that CO_2 may not be desorbed spontaneously and that it inhibits the reaction rate. Winter [14] studied the oxidation of CO over Cu_2O and confirmed the presence of CO_2 in the gas desorbed from the catalyst after an experiment. The catalyst was active in oxygen exchange with CO and CO_2 but only 10% of heavy oxygen from the labelled oxide appeared in CO_2 during CO oxidation. Stone [30] attributed the results of Winter's oxygen, was playing the major role during the catalysis.

Calorimetric measurements have, in fact, provided additional evidence in favour of the scheme represented by equation (7) to (10). When admitting CO to a cobaltous oxide surface at which oxygen had presorbed, the heat of adsorption gradually fell for the first few incremental doses, but no CO_2 was desorbed. Another few incremental additionals, however, caused the heat of adsorption to fall drastically by as much as 20 kcal mole^{-1} with the concomitant formation of gaseous CO_2. From the two thermochemical equations (4) and (5), written here again for convenience;

$$CO\ (g) + 2O\ (ads) = CO_3\ (ads) + 60\ kcal \qquad (4)$$

$$CO\ (ads) = CO\ (g) \quad - 20\ kcal \qquad (5)$$

the heat of formation of the CO_3 complex is 40 kcal mole^{-1};

$$(4)+(5); \qquad CO\ (ads) + 2O\ (ads) = CO_3\ (ads) + 40\ kcal \qquad (9a)$$

Now the standard heat of formation of CO (g) is 27 kcal mole^{-1};

$$C + 1/2O_2\ (g) = CO\ (g) + 27\ kcal \qquad (11)$$

and rewriting equation (1) for the adsorption of oxygen;

$$1/2O_2\ (g) = O\ (ads) + 28\ kcal \qquad (1)$$

the standard heat of formation of the CO_3 complex may be computed from Hess's law;

$$\{2X(1)\}+(9a)+(11)-(5); C + 3/2O_2(g) = CO_3\ (ads) + 143\ kcal \qquad (12)$$

Recalling that the standard heat of formation of CO_2 (g) is 94 kcal mole^{-1};

$$C + O_2\ (g) = CO_2\ (g) + 94\ kcal \qquad (13)$$

the heat of reaction when gaseous CO gaseous CO is admitted to a surface containing the CO_3 complex must be 18 kcal;

2X(13)-(12)-(11);$CO_3(ads)+CO(g) = 2CO_2(g) + 18$ kcal (10a)

From these thermochemical considerations, it appears that the decrease in heat of adsorption to be expected when reaction (10) takes over from reaction (9) is 40 - 18 = 22 kcal, in close agreement with the observed value of 20 kcal.

For nickel oxide the heat of formation of the surface CO_3 complex is greater than for either CoO or Cu_2O. Because of this increase in the heat of formation, reaction (10), in which CO_2 is formed by the interaction of the complex with gaseous CO, is now endothermic and is susceptible to the effects of poisons. Such a poisoning effect has been noted by Winter [14]. The decreased activity of NiO is thus explained in such terms. Some activity is possible, however, by the reactants utilizing an alternative reaction path involving an Eley-Rideal mechanism. Thus Teichner and coworker [37,41] have explained their results using high area by supposing that NiO in terms of a Rideal-type mechanism in which the CO_3 complex is decomposed by gaseous CO and so affording a possible alternative route for the co-workers [42], using high area NiO prepared at a relatively low temperature showed that the product CO_2 inhibits the reaction rate. When incremental doses of CO were admitted to NiO, in which oxygen had been presorbed, the calorimetric heat of adsorption at half coverage was 70 kcal/mole. Since NiO is a p-type semiconductor and the adsorption of oxygen is cumulative, an increase in the number of positive holes results, thus increasing the conductivity of the oxide. When oxygen is adsorbed, the heat evolved at half coverage is 10 kcal/mole and the first step in the adsorption sequence is written;

$$Ni^{2+} + 1/2O_2\ (g) \quad = \quad O^{-}\ (ads) + Ni^{3+} + 10\ kcal \qquad (14)$$

The subsequent step in which CO interacts with the adsorbed oxygen can either be written as single process in which CO_2 is spontaneously desorbed or as two distinct step;

$$Ni^{3+} + O^{-}(ads) + CO\ (g) \quad = \quad CO_2\ (ads) + Ni^{2+} + 70\ kcal \qquad (15)$$

$$CO_2\ (ads) \quad = \quad CO_2\ (g) - 15\ kcal \qquad (16)$$

By addition of equations (14), (15) and (16) the heat of combustion of gaseous CO appears to be 65 kcal mole^{-1}. Thus, Teichner considered CO_2 to be adsorbed at the surface of the oxide. Supporting evidence for reaction (15) is indicated by a change in colour of the nickel oxide from black to yellow (indicating a change in the defect structure of the solid) and the fact that no CO_2 was detected in the gas phase.

Teichner and co-worker [42] also examined calorimetrically two other reaction sequences. CO was adsorbed on freshly prepared NiO and then exposed to gaseous oxygen. The initial heat of adsorption was 134 kcal mole^{-1}, at half coverage was 115 kcal mole^{-1}, and gradually decreased thereafter. The reaction proposed to account for these observations may be written;

$$CO\ (ads) + O_2\ (g) \quad = \quad CO_3\ (ads) \qquad (17)$$

Next, gaseous CO was admitted to the catalyst at which the surface complex had been preformed. The initial heat of adsorption was 65 kcal mole^{-1} falling to 40 kcal mole^{-1}. At the same time the conductivity of the sample decreased and the solid turned from black to yellow. Gaseous CO_2 was also detected. By writing down the thermochemical equations, it is possible to demonstrate that at the most active part of the surface neither gaseous nor adsorbed CO_2 could be produced. On the part of the surface where the heat of reaction is approximately 100 kcal mole^{-1}, the thermochemical data are accounted for by adsorbed CO_2 being fromed at the surface by the reaction;

$$CO_3\ (ads) + CO \quad = \quad 2CO_2\ (ads) + 100\ kcal \qquad (18)$$

The conductivity would also fall, since the number of positive hole units $Ni^{3+} - Ni^{2+}$ decreases, but no gaseous CO_2 would be released. Teichner and co-workers [42] believed that adsorbed CO_2 is produced by that part of the surface at which the heat of reaction is 100 kcal mole^{-1} or less: it is also possible to demonstrate that gaseous CO_2 is formed by that part of the surface which reacts with a heat of approximately 40 kcal mole^{-1}. Thus, the only combination of thermochemical equation which satisfies the formation of both adsorbed and gaseous CO_2 are;

$$CO\ (ads) + O_2 \quad = \quad CO_3\ (ads) + 100\ kcal \qquad (19)$$

$$CO_3\ (ads) + CO \quad = \quad 2CO_2\ (ads) + 65\ kcal \qquad (20)$$

and

$$CO_2\ (ads) + O_2 \quad = \quad CO_3\ (ads) + 40\ kcal \qquad (21)$$

$$CO_3\ (ads) + CO \quad = \quad 2CO_2\ (g) + 65\ kcal \qquad (22)$$

The average heats of adsorption of CO (g) and CO_2 on the NiO powder used are 29 kcal mole^{-1} and 31 kcal mole^{-1}, respectively;

$$CO\ (g) \quad = \quad CO\ (ads) + 29\ kcal \qquad (23)$$

$$CO_2(g) \quad = \quad CO_2\ (ads) + 31\ kcal \qquad (24)$$

It is therefore easy to see that both sets of equations conform to the accepted value for the heat of combustion of CO, viz. 67 kcal mole^{-1};

$$1/2\{(19)+(20)+(23)\}-(24);\ CO(g)+1/2O_2(g) = CO_2(g) + 66\ kcal \quad (25)$$

$$1/2\{(21)+(22)+(23)\};\qquad CO(g)+1/2O_2(g) = CO_2(g) + 67\ kcal \quad (26)$$

It would be interesting to monitor, mass spectrometrically, the gaseous CO_2 formed and to note at what stage in the reaction it is released from the surface. Kinetic measurements made by Teichner during the reaction established that the slow stage in the ratio is the desorption of gaseous CO_2, and hence the electronic structure of the solid has no influence on the catalytic activity. This latter deduction is confirmed experimentally. However, it does not accord with the observation of Dry and Stone [43] and of Roginskii and co-worker [44], in which it was shown that the apparent activation energy varied with the addition of foreign ions. At temperatures below 350 °C the addition of lithium ions increased the activation energy, while at temperature above 300 °C the addition of lithium ions decreased the activation energy. With regard to such a reversal of behaviour at high and low temperature, Stone concluded that it is likely that one or other of the species participating in the reaction is adsorbed more strongly than by the pure oxide and that the electronic boundary layer theory is not the correct premise on which to base an argument.

To summarize, it may be said that there are some measures of agreement in that CO_2 poisons the reaction at low temperature and that such a prediction cannot be made on the basis of the electronic theory of catalysis. Of greater significance is the fact that a compensation effect operates and this poses the following dilemma. It seems to be a paradox that a change in the lattice which considerably increases the positive hole concentration, and hence the activation energy, also decreases the Arrhenius frequency factor. If the reaction between adsorbed CO and lattice oxygen is rate-determining, the apparent activation energy will contain a contribution from the heat of adsorption, and if this varies with alternation in the Fermi level, so also will the activation energy.

3.4 Supports and Metal-Support Interactions in Catalyst Design [45]

3.4.1 Introduction

Catalysts involving group VIII metals are usually prepared by dispersing the metal onto a high surface area support, to assure that a high proportion of the metal atoms is available for interaction with gaseous reactants. For most industrial applications, supports are sought which possess high surface area, high thermal and high chemical stability, and high mechanical strength. While it was originally thought that the support was simply an inert carrier of the active component, work conducted in the late 1950s by Schwab (1978) and Solymosi (1967) revealed that significant changes in the catalytic properties of a metal could be achieved by varying support composition. Extensive evidence supporting this view has appeared over the past 7 years, engendered by an interest in the so-called strong metal-support interaction (SMSI) reported by Tauster and coworkers at Exxon (Tauster, Fung, and Garten, 1978; Tauster and Fung, 1978; Tauster, Murrell, and Fung, 1979).

3.4.2 Classification of Metal-Support Interaction

For a given metal, variations in support composition can influence the size and morphology of the supported metal particles, the surface electronic properties of the particles and the nature of the sites present at the points of contact between the metal and the support. Only the latter two of these three effects should properly be attributes to metal-support interactions, since changes in particle size and morphology can be achieves in other ways (e.g., sintering, redispersion). Thus, we might refer to changes in particle size and morphology with support composition as a nonspecific effect and refer to all other changes as specific effects of support composition.

The distinctions between specific and nonspecific effects of support composition are particularly important to recognize for structure-sensitive reactions (Bond, 1982). For such reaction, the overall changes in the activity and selectivity of a given metal upon changing support may be due only in part to the alteration of support composition, the balance being due to changes in particle size and/or morphology. To properly assess the influence of metal-support interactions for structure-sensitive reactions, it is therefore, necessary to know a priority the degree to which specific activity and selectivity are influenced by metal dispersion. Unfortunately, though, much of the recent literature on metal-support interactions has failed to distinguish between the effects of particle size and specific supports. This has made it difficult to compare the results of different authors and to properly quantify the magnitude of specific support effects for various metal-support systems.

3.4.3 Influence of Metal-Support Interactions on Adsorptive Properties

The influence of metal-support interactions on the chemisorption of H_2 and CO has been investigated for virtually all of the group VIII metals. It is generally observed that an increasing degree of metal-support interaction is manifested by a decrease in H_2 and CO chemisorption capacity with increasing temperature of catalyst reduction. An illustration of this effect is shown in Figure 3.7 for H_2 chemisorption on Ir. It is significant to note that the strongest suppressions of H_2 chemisorption is observed for the oxides of Nb, Mn, V, Ta, and Ti, all of which can be reduced more readily than the remaining oxides listed in Figure 3.7 (Tauster et al., 1981). This correlation suggests that the creation if anionic vacancies in an oxide facilitates the migration of oxidic moieties onto the surface of the supported metal particles. The validity of this interpretation is supported by the work of Resasco and Haller(1983), which shows that the chemisorption capacity of Rh/TiO_2 decreases proportionally with the surface diffusion of TiO_x species. Further substantiation of the decoration model of chemisorption suppression comes from the observation that similar effects are observed with small as well as large metal

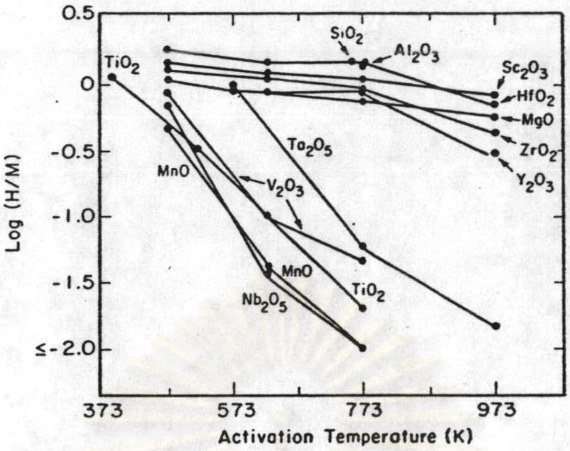

Figure 3.7 Hydrogen chemisorption on Ir supported on various oxides as a function of activation in hydrogen for 1 hr at various temperatures. H/M = atomic ratio of hydrogen adsorbed to Ir in catalyst. From Tauster et al. (1981).

particles. If, for example, the modification in chemisorption behavior were due solely to interactions occurring at the point of metal-support contact, then the influence of such interactions on large particles would be expected to be smaller than that observes for small particles.

The means by which metal oxide moieties present on the surface of metal particles alter the chemisorptive properties of the metal particles is not yet fully understood. It is obvious that the primary effect is simple site blockage, but there is now growing evidence that metal sites adjacent to metal oxide moieties might also by affected. An illustration of this is shown in Figure 3.8 for the case of TiO_x deposited on the surface of a Rh foil. With increasing TiO_x coverage, the CO chemisorption capacity falls off more rapidly than would be predicted by simple site blockage.

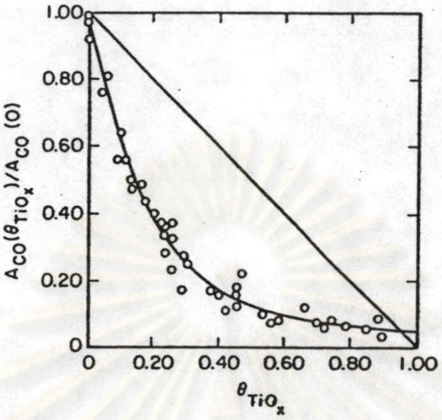

Figure 3.8 Normalized CO adsorption capacity of a Rh foil decorated with TiO_x, as a function of TiO_x coverage. Adsorption temperature 298 K. From Levin et al. (1985).

Levin et al.(1986a) have demonstrated that the data can be explained by assuming that CO chemisorption is suppressed on those sites that are immediately adjacent to the TiO_x islands covering the surface of the Rh foil, in addition to those Rh sites covered by the TiO_x islands. The authors postulate that the Rh sites along the perimeter of the TiO_x islands are affected by a perturbation in the density of states at the Fermi level, along the lines described by Feibelmann and Hamann (1984,1985).

In addition to altering the chemisorptive capacity of a metal oxide moieties may also alter the distribution of adsorption states. Two cases are illustrated in Figures 3.9 and 3.10. In both instances the chemisorptive properties of Pd/SiO_2 have been altered by the promotion of the catalyst with TiO_x. It is evident from both

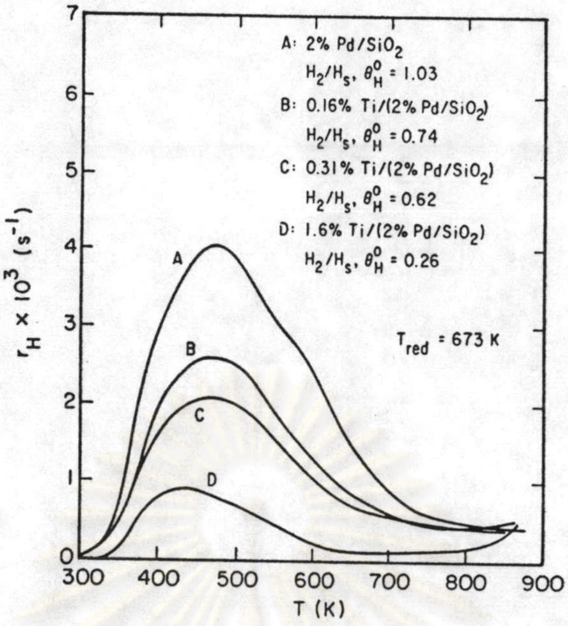

Figure 3.9 Temperature-programmed desorption spectra for H_2 adsorbed on Pd/SiO_2 and TiO_2-promoted Pd/SiO_2. From Reick and Bell (1985)

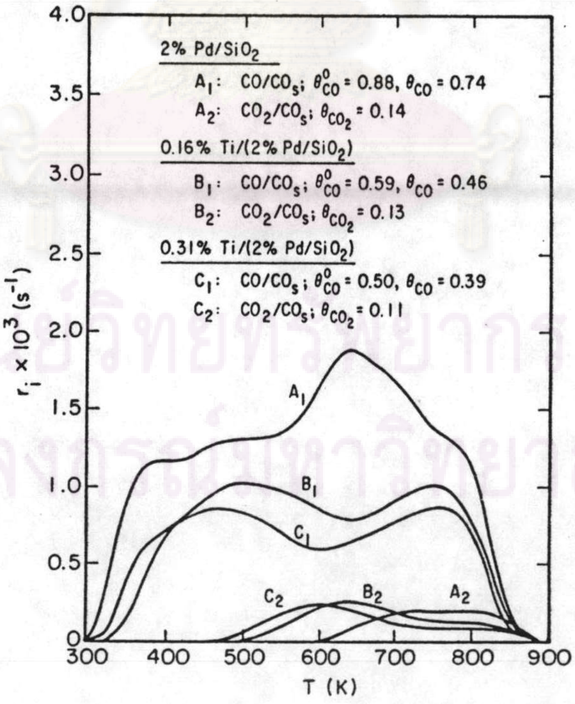

Figure 3.10 Temperature-programmed desorption spectra for CO adsorbed on Pd/SiO_2 and TiO_2-promoted Pd/SiO_2. From Rieck and Bell (1985).

figures that with increasing addition of TiO_x, the initial level or CO chemisorption, given by θ_H or θ_{CO}, decreases. While TiO_x promotion appears to have no effect on the distribution of H_2 adsorption states, the distribution of CO adsorption states is affected significantly. The most pronounced effect is the preferential suppression of CO chemisorption on Pd(100) surfaces, characterized by the peak at 630 K. A further effect of TiO_x promotion is the shift in the onset of CO_2 formation to lower temperatures. Since CO_2 is formed via CO dissociation and subsequent reaction of the released oxygen atom, the downscale shift in the CO_2 peak is evidence of an enhancement in the case of CO dissociation.

3.4.4 Strong Metal-Support Interaction [46]

It was observed that the reduced support interacts so strongly with noble metal that it lowers the precious metals H_2 chemi-adsorption capacity at room temperature.

Figure 3.11 shows the result of reduction of oxidation of Pt-supported on TiO_2 at 400-500 °C under hydrogen or oxygen atmosphere. It is evident that as TiO_2 reduces, the H_2 uptake decreases; as reduced TiO_2 is oxidized, the H_2 uptake increases. This is also observed for Pt/Al_2O_3 reduced and oxidized at 400-500 °C in hydrogen or oxygen atmosphere, respectively. When Pt/Al_2O_3 or Pt/TiO_2 are reduced at high temperatures, the hydrogen adsorption capacity for Pt is greatly reduced. This is known as the SMSI phenomenon (strong metal support interaction). There are two explanations for SMSI:

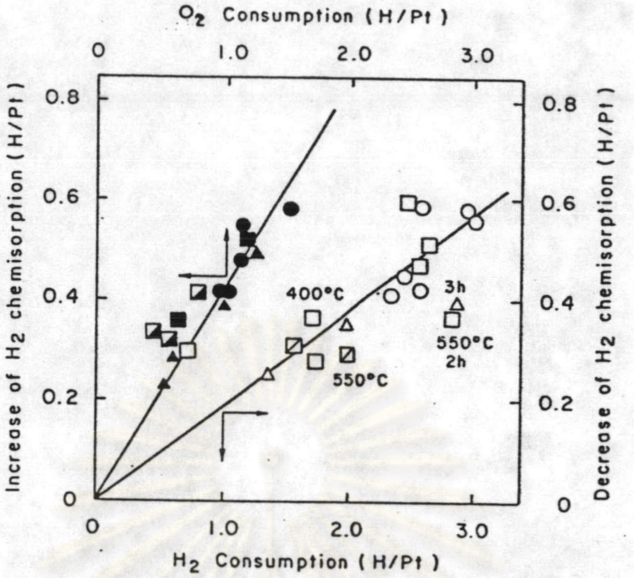

THE DECREASE OF H_2 CHEMISORPTION VS THE AMOUNT OF THE H_2 CONSUMPTION AND THE INCREASE OF H_2 CHEMISORPTION VS THE AMOUNT OF O_2 CONSUMPTION. UNLESS OTHERWISE STATED, EACH TREATMENT (IN H_2 AT 500°C AND IN O_2 AT 400°C) WAS CARRIED OUT AT THE GAS PRESSURE OF 50 TORR FOR 1h (◩▨ ; THE GAS PRESSURE WAS ABOUT 5 TORR)

Figure 3.11 Result of reduction of oxidation of Pt supported TiO_2 at 400° - 500°C under hydrogen or oxygen atmosphere.

1. Pt alloys with reduced aluminum or titanium and losses its hydrogen adsorption capacity.
2. The reduced titanium or aluminum oxide becomes an n-type electrical conductor (semiconductor or insulator) and transfers electrons to Pt. This reduces the hydrogen uptake capacity of Pt.

The latter explanation is preferred.

In another study, three samples were prepared by impregnation of TiO_2 with Pt, Rh, and Ni. A fourth sample was prepared without any metal. The electrical conductivity of the four samples was measured under the following conditions: catalyst treatment at 200 °C temperature, 250 torr H_2 pressure, then evacuation at 400°C, followed by reducing the temperature to 25 °C, and finally introducing H_2 at 50, 100, and 150 torr pressure.

The data indicate that TiO_2, after evacuation, behaved as degenerate semiconductor with low activation energy. However, metal, which is the primary source of hydrogen spillover, partially reduces the TiO_2 under hydrogen atmosphere. The hydrogen donates electrons to TiO_2 and increases conductivity. After evacuation at 400 °C, the reverse takes place, and TiO_2 loses electrons, thus reducing conductivity due to reverse spillover. Reducing the temperature from 400°C to 25°C reduces conductivity by an order of magnitude. This is an activating process with activation energy of 8 kcal/mole. The addition of H_2 increases the conductivity at 25°C. Hydrogen behaves as a donor impurity and converts to H^+, which accounts for the increased conductivity.

In the evacuation step at 400°C, hydrogen is removed by reverse spillover,

$$H^+ + e^- \rightleftharpoons H^\cdot$$

$$2H^\cdot \rightleftharpoons H_2,$$

and TiO_2 conductivity decreases (see Figure 3.12). The reduced Pt/TiO_2 has high electron density and low hydrogen uptake capability. The reverse is true with an oxidized catalyst. This indicates that SMSI is due to increased electron density of TiO_2 and, possibly, the transfer of electrons to Pt crystallites.

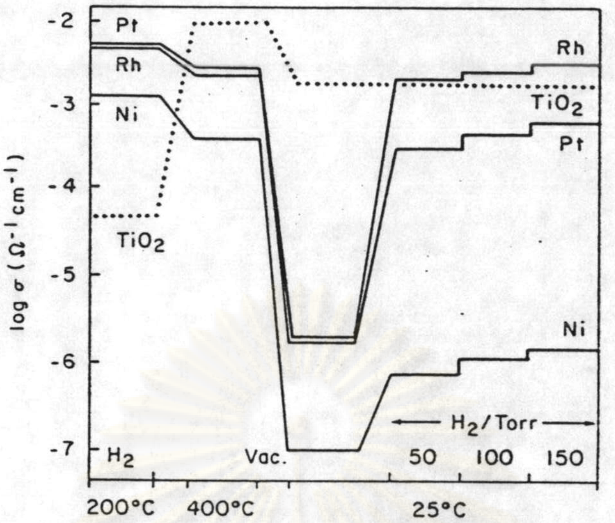

Figure 3.12 Electrical conductivity of TiO_2 and of Pt, Rh, and Ni/TiO_2 under indicated conditions.

Figure 3.13 shows Rh/TiO_2 conductivity versus H_2 (lower scale) and H_2 1/2 (upper scale) partial pressure. The data confirm the theory that adsorbed H donates electrons to Rh/TiO_2. It has been shown that TiO_2 is reduced by a beam of H atoms generated by a microwave discharge or by hydrogen spillover produced by Rh. In both case, the TiO_2 surface is reduced. Reduced titanium oxide behaves as n-type semiconductor with increased electropotential (Fermi energy). The increase of electropotential and transfer of electrons to noble metal prevents the noble metal from adsorbing H at room temperature. This condition is favorable for the creation of SMSI between metal and TiO_2. SMSI has been observed between Pt/Al_2O_3, Pt/$ZnAl_2O_3$, and others.

Strong metal-support interaction was reported in 1978 for Pd/TiO_2. The catalyst was reduced at 500 °C in a hydrogen atmosphere. After evacuation, the catalyst was cooled to room

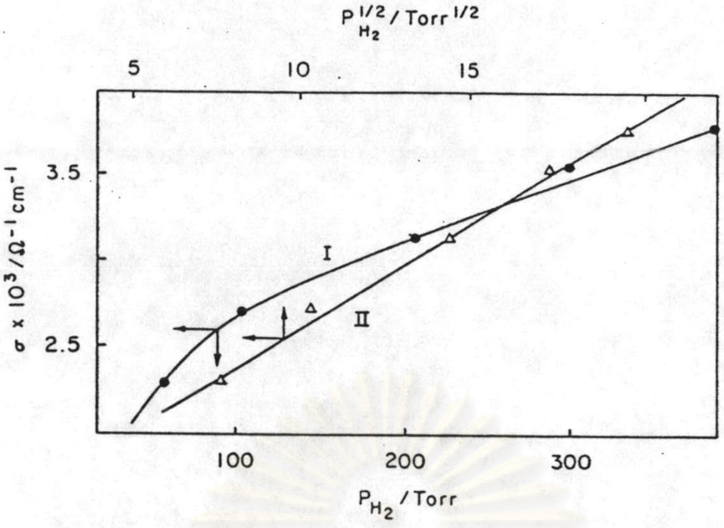

Figure 3.13 Rh/TiO_2 conductivity isotherm as a function of P_{H2}(I) and linear transform (II).

temperature. It was found that Pd catalyzed the reduction of TiO_2 with the result that there was a significant loss of H_2 or uptake capacity. This property is also known as SMSI. However, the SMSI does not affect catalytic activity significantly. The SMSI is normally associated with partial reduction of oxides and increases their electron density of semiconductor or insulator oxides. SMSI occurs with other noble metals and most oxides and zeolites.

In the presence of spillover hydrogen, stoichiometric metal oxides reduce to a nonstoichiometric oxidation state. Some oxides lose all their oxygen and reduce to a metallic state. This depends on the temperature of reduction and the specific oxide. Hydrogen spillover lowers the reduction temperature of oxides significantly. Pt and Pd are most effective in this case. A large number of metal oxides have been reduced by spillover from Pt or Pd, at a much lower temperature than is the case when the reductant is molecular H_2. The metals are Co_3O_4, V_2O_5, VO_3, Fe_2O_3, WO_3, Re_2O_7, CrO_4, Ni_3O_4, MnO_2, NiO, CuO, Cu_2O, ZnO, SnO_2, and Ag_2O. SMSI takes place between many metals and metal oxides. They usually do not lose their catalytic activity, but they may lose CO and H_2 uptake capability. It is important to mention that reduced metal oxides have oxygen vacancies, and their SMSI property frequently is reversed with oxidation.

3.4.5 Influence of reduced oxides on the properties of transition metals [47]

It was first reported about ten year ago that certain transition metal oxides can have a dramatic effect on the chemisorptive and catalytic properties of metals when they are in close contact with the metal. This effect was originally termed Strong Metal-Support Interaction, but is currently referred to as decoration effect. The first report of this effect was on the suppression of hydrogen and carbon monoxide adsorption capacity of noble metals. It has been found that when a noble metal is supported on TiO_2, the material chemisorbs H_2 or CO at a stoichiometry of roughly one H atom or CO molecule per surface exposed noble metal atom, if the material is reduced at 200 °C. If the material is reduced at 500 °C, its ability to chemisorb H or CO is essentially completely suppressed. This is illustrated with typical data in Table 3.5. It was later found that this effect is not unique to TiO_2 as the support. Figure 3.14 shows the extent of suppression of the hydrogen chemisorptive capacity as a function of reduction temperature for various oxide supports. In general, oxides that are readily reducible at intermediate temperatures all show this effect. The effect is reversible. That is, reoxidation with oxygen followed by a low temperature reduction at 200 °C restores most of the adsorptive capacity.

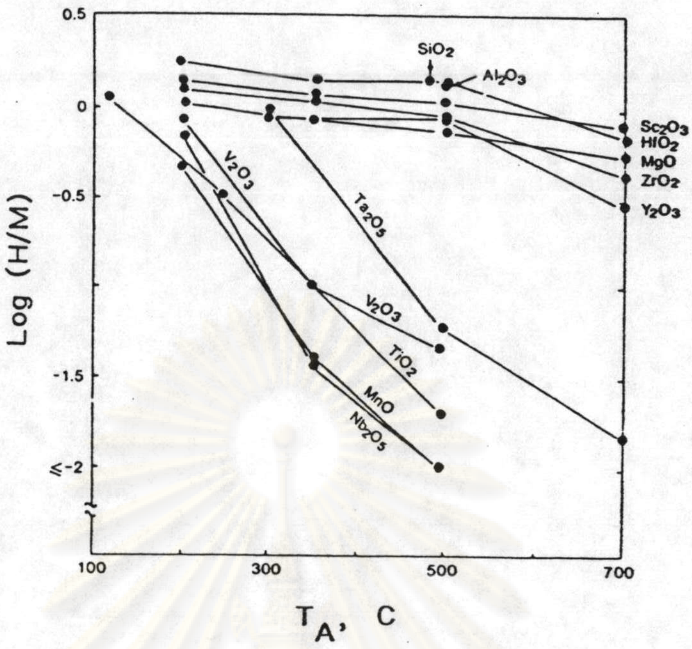

Figure 3.14 Hydrogen chemisorption on iridium supported on various oxides as a function of activation in hydrogen for 1 h at each of various temperatures. T_A is the activation temperature, and H/M is the atomic ratio of hydrogen adsorbed to iridium in the catalyst. (From Science, **211**, 1121 (1981), copyright American Association for the Advancement of Science).

The influence of the decoration effect on the catalytic properties of the metal depends on the reaction. Some typical examples are shown in Table 3.6. It can be seen that the decoration effect suppresses the activity of Pt for benzene hydrogenation and cyclohexane dehydrogenation, but enhances the activity in CO hydrogenation. The activity of the Fe catalyst in ammonia synthesis is slightly decreased, but the activation energy is greatly increased. In the case of butane hydrogenolysis, the selectivity and the activity are both altered.

Table 3.5 Suppression of H_2 Adsorption Capacity due to Decoration Effect. (From Science, **211**, 1121 (1981), copyright American Association for the Advancement of Science).

2% Metal on TiO_2 Supported	H atom adsorbed/Total metal atoms Reduction at 200 °C	 Reduction at 500 °C
Ru	0.23	0.06
Rh	0.71	0.01
Pd	0.93	0.05
Os	0.21	0.11
Ir	1.60	0.00
Pt	0.88	0.00

In addition to these examples, it has been shown that CO hydrogenation on Ni catalysts is also enhanced by the decoration effect, although the extent of enhancement may vary from very little to rather substantial. In ethane hydrogenolysis on titania-supported Rh, it has been found that the activity decreases rapidly with increasing reduction temperature (Figure 3.15), whereas the cyclohexane dehydrogenation activity over the same catalyst remains almost unchanged.

It is now rather well established that this effect is not due to the formation of alloy (e.g. Pt-Ti alloy), the encapsulation of the metal by the support, sintering of the metal, poisoning of metal by impurities in the support, or simply electron transfer between the bulk of the support and the bulk of the metal

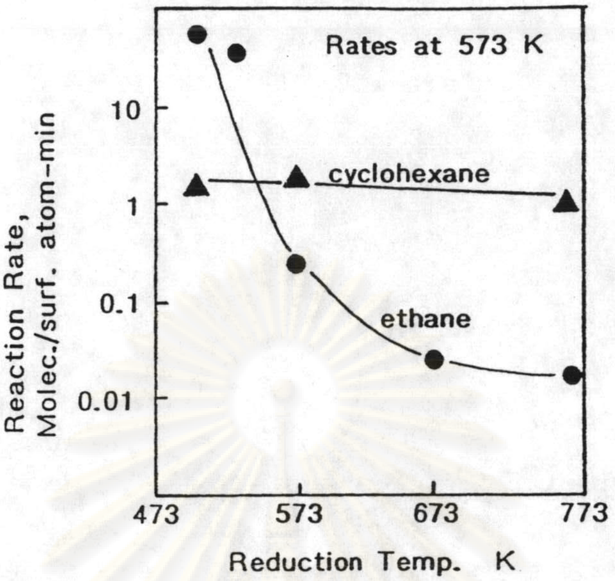

Figure 3.15 Ethane hydrogenolysis and cyclohexane dehydrogenation on Rh/TiO_2 catalyst as a function of catalyst reduction temperature. (From J.Catal., **82**, 279 (1983), copyright Academic Press).

crystallite. These conclusions follow from a variety of experimental observations.

For example, transmission electron microscopic studies as well as X-ray diffraction show no evidence of sintering, and Mossbauer spectroscopy shows that the bulk of the iron crystallites is the same whether or not the sample is exhibiting the decoration effect, even though the titania support near the metal crystallite is reduced from TiO_2 to Ti_4O_7.

The current picture is that the origin of the effect is the migration of small particles of reduced titania (or other

Table 3.6 Effect of Decoration on the Catalytic Properties of Noble Metals

Reaction	Catalyst	Reaction Rate	Other Effects
C_6H_6 hydrogenation at 288 K	4.8% Pt/TiO_2		
	523 K reduced	40 mmole/h-g cat.	
	773 K reduced	3.5 mmole/h-g cat.	
C_6H_{12} dehydrogenation at 523 K	2.7% Ir/TiO_2		
	523 K reduced	1400 mmole/h-g cat.	
	773 K reduced	304 mmole/h-g cat.	
CO hydrogenation at 524 K	1.9% Pt/TiO_2		
	473 K reduced	0.0111 molecules/s-Pt_s	
	773 K reduced	0.076 molecules/s-Pt_s (0.0195 if assumed the same dispersion as low-temperature reduced sample)	
NH_3 synthesis at 673 K	1.14% Fe/TiO_2		
	713 K reduced	0.031 ks^{-1}	Eact=100 kJ $mole^{-1}$
	798 K reduced	0.011 ks^{-1}	Eact=220 kJ $mole^{-1}$
C_4H_{10} hydrogenolysis at 623 K	4.8% Pt/TiO_2		
	623 K reduced	Relative product formation rate: C_1=35, C_2=47, C_3=25, i-C_4=88	
	773 K reduced	C_1=0.65, C_2=1.1, C_3=0.7, i-C_4=0	

reduced support) onto the metal crystallites to "decorate" the metal surfaces. These decorating reduced oxide particles may partially block the metal surfaces from gas molecules, affect the electronic structure of the neighboring metal atoms, or provide an oxide-metal interface for interaction with molecules. Depending on the reaction, one or more of these effect may participate to affect the observed characteristics of the reaction.

That decoration is the physical picture was first suggested by Dumesic on the Fe/TiO_2 system. Using Mossbauer spectroscopy, it has been observed that the bulk properties of Fe crytallites are the same whether they are in the decorated state or not. Thus the effect must be a surface phenomenon. It is then proposed that titania species cover the iron crytallites. Such a decoration model would suggest that the extent of the effect should depend on the time allowed for the reduced oxide particles to migrate onto the metal crystallites and the interface between the metal and the oxide. These have been confirmed. It is observed that using the rate of ethane hydrogenolysis as a measure, the extent of the decoration effect depends linearly on the square root of the reduction time, which is characteristic of diffusion processes. For a given reduction time, the hydrogenolysis activity decreases as the inverse of the particle diameter. Finally, the increasing suppression of the hydrogenolysis activity as the reduction time increases is found to parallel a similar suppression by the addition of copper to a nickle catalyst, which is interpreted by the breaking-up of nickle ensembles on the surface by copper atoms. Thus the data are consistent with the model that the surface metal ensembles are broken up by reduced titania particle decorating the surface.

Recently, it has been further proposed that the metal-oxide interaction occurs through the interaction of metal atoms with oxygen ion lattice vacancies in the reduced oxide. At temperatures sufficiently high to induce the decoration effect, the oxide support is reduced so that it has a high concentration of anion vacancies. The high concentration of anion vacancies enhances the diffusion of metal atoms into the near-surface region of the bulk, and results in the formation of a raft-like metallic cluster covered by a thin (atomic) layer of the support. When the support is reoxidized, the anion vacancies are filled, driving the metal atoms back to the surface.

When titania particles are deposited on model catalysts of a Ni (111) single crystal surface or a Pt foil, a similar suppression of the H_2 or CO chemisorption capacity is observed which is similar to that resulting from high temperature reduction of supported metals. Enhanced catalytic activity in CO hydrogenation has also been observed on these low surface area catalysts. In the case of Pt foil, the activation energy is reduced from 126 to 80 kJ/mole. Furthermore, a small amount of deposited TiO_x particles is found to enhance the methanation of Ni. At an optimum coverage of 8%, (recently there is doubt about this number because of questions about the calibration method employed), the activity is four times that of a clean Ni surface. On the other hand, complete suppression of the chemisorptive capacity requires complete coverage of the metal surface by the oxide particles.

The extent of election transfer between the metal and the decorating particles is not established. For example, a study of Pt crystallites supported on a TiO_2 single crystal surface by XPS and AES suggests electron transfer from TiO_2 to Pt, while a XANES study suggests electron transfer from Pt to TiO_2.

The influence of the decorating effect on the heat of adsorption depends on the system. On Pt supported on titania, the effect results in a decrease in the initial heat of adsorption of H_2 from 92 to 82 kJ/mole, but no change for CO adsorption. The integral heats of adsorption of both CO and H_2 are substantially reduced. However, the integral heat of adsorption of CO and H_2 on Pd is not affected.